J Fluoresc (2012) 22:261–267
DOI 10.1007/s10895-011-0956-6

ORIGINAL PAPER

# Design and Synthesis of a Terbium(III) Complex-Based Luminescence Probe for Time-Gated Luminescence Detection of Mercury(II) Ions

**Guanfeng Cui · Zhiqiang Ye · Run Zhang · Guilan Wang · Jingli Yuan**

Received: 9 June 2011 / Accepted: 10 August 2011 / Published online: 20 August 2011


**Abstract** Time-gated luminescence detection technique using lanthanide complexes as luminescent probes is a useful and highly sensitive method. However, the effective application of this technique is limited by the lack of the target-responsive luminescent lanthanide complexes that can specifically recognize various analytes in aqueous solutions. In this work, a dual-functional ligand that can form a stable complex with $Tb^{3+}$ and specifically recognize $Hg^{2+}$ ions in aqueous solutions, *N,N,N*$^{1}$,*N*$^{1}$-{[2,6-bis(3′-aminomethyl-1′-pyrazolyl)-4-[*N,N*-bis(3″,6″-dithiaoctyl)-aminomethyl]- pyridine]} tetrakis(acetic acid) (BBAPTA), has been designed and synthesized. The luminescence of its $Tb^{3+}$ complex is weak, but can be effectively enhanced upon reaction with $Hg^{2+}$ ions in aqueous solutions. The luminescence response investigations of BBAPTA-$Tb^{3+}$ to various metal ions indicate that the complex has a good luminescence sensing selectivity for $Hg^{2+}$ ions, but not for other metal ions. Thus a highly sensitive time-gated luminescence detection method for $Hg^{2+}$ ions was developed by using BBAPTA-$Tb^{3+}$ as a luminescent probe. The dose-dependent luminescence enhancement of the probe shows a good linearity with a detection limit of 17 nM for $Hg^{2+}$ ions. These results demonstrated the efficacy and advantages of the new $Tb^{3+}$ complex-based luminescence probe for the sensitive and selective detection of $Hg^{2+}$ ions.

G. Cui · Z. Ye (✉) · R. Zhang · G. Wang · J. Yuan (✉)
State Key Laboratory of Fine Chemicals, School of Chemistry,
Dalian University of Technology,
Dalian 116024, People's Republic of China
e-mail: zhiqiangye2001@yahoo.com.cn
e-mail: jingliyuan@yahoo.com.cn

**Keywords** Luminescent probe · Terbium complex · Mercury ions · Time-gated luminescence detection

## Introduction

As one of heavy metal ions, $Hg^{2+}$ can cause severe health problems to human beings when it is ingested or inhaled due to its high toxicity [1–3]. The excessive exposure of the body to mercury can lead to neurological diseases, mitosis impairment, DNA damage and nervous system defects [4–6]. Mercury is present in many environments, either as a naturally occurring species or as a by-product of manufacturing and industrial processes, such as oceanic and volcanic emission, solid-waste incineration, gold mining and combustion of fossil fuel [7–10]. Thus, its contamination is a global problem that has received considerable attention from the industrial and biological points of view. Due to the above imperilment, the implementation of securing the health and safety requires the availability of rapid, selective and sensitive methods to detect the concentration of mercury in environmental and biological systems.

To date, a variety of analytical methods have been developed for the detection of $Hg^{2+}$, such as atomic absorption spectroscopy, fluorescence spectrometry, gas chromatography, high performance liquid chromatography and capillary electrophoresis [11–15]. Fluorometric assays using a fluorescent probe that can specifically respond to $Hg^{2+}$ are considered to be one of the most promising methods due to its high sensitivity, selectivity, experimental convenience and availability for living systems. Towards this end, a number of fluorescent probes for the detection of

$Hg^{2+}$ have been developed in recent years [16–22]. Unfortunately, in terms of actual applicability, most of the reported fluorescent probes have one or more limitations, such as poor aqueous solubility, interference from other metal ions, strict reaction condition, slow response to $Hg^{2+}$ or complicated synthetic route.

Herein we describe the design and synthesis of a unique $Tb^{3+}$ complex-based luminescent probe for highly selective and sensitive time-gated luminescence detection of $Hg^{2+}$ ions. By incorporating a $Tb^{3+}$ chelating moiety, a polyacid derivative of 2,6-bis(N-pyrazolyl) pyridine that has an good antenna capability for sensitizing the $Tb^{3+}$ emission [23–25], with a $Hg^{2+}$ chelating moiety, 3,6,12,15-tetrathia-9-monoazaheptadecane (TTM), a novel dual-functional ligand that can simultaneously coordinate with $Tb^{3+}$ and $Hg^{2+}$ ions in aqueous buffers, *N,N,N*$^{1}$,*N*$^{1}$-{[2,6-bis(3′-aminomethyl-1′-pyrazolyl)-4-[*N,N*-bis(3″,6″-dithiaoctyl)-aminomethyl]- pyridine]} tetrakis(acetic acid) (BBAPTA), was successfully synthesized (Scheme 1). Because the TTM moiety in the ligand is a reactive switch capable of quenching the excited state of the $Tb^{3+}$-2,6-bis(N-pyrazolyl) pyridine complex via a photo-induced electron transfer (PET) process, the luminescence of BBAPTA-$Tb^{3+}$ complex is weak. However, in the presence of $Hg^{2+}$, due to the high affinity of TTM to $Hg^{2+}$, a heterobimetallic complex $Hg^{2+}$-BBAPTA-$Tb^{3+}$ is formed, which makes the PET process from TTM to the $Tb^{3+}$-complex moiety be inhibited, and thereby, the intra-molecular energy transfer from the antenna ligand to $Tb^{3+}$ is feasible, and the long-lived $Tb^{3+}$ luminescence is turned on (Scheme 1). Moreover, since the coordinating affinities of the TTM moiety to other metal ions are rather weak in aqueous solutions [26], the "off-on" luminescence response of BBAPTA-$Tb^{3+}$ to $Hg^{2+}$ can be expected to be used for the highly selective luminescence detection of $Hg^{2+}$ ions even in the presence of other metal ions.

## Experimental

### Materials and Physical Measurements

3,6,12,15-Tetrathia-9-monoazaheptadecane (TTM) was synthesized by using a literature method [26]. Tetraethyl *N,N,N*$^{1}$,*N*$^{1}$-[2,6-bis(3′-aminomethyl-1′-pyrazolyl)-4-hydroxymethyl-pyridine] tetrakis(acetate) (compound 1) was synthesized according to our previous method [27]. Tetrahydrofuran (THF) and acetonitrile were used after appropriate distillation and purification. Unless otherwise stated, all chemical materials were purchased from commercial sources and used without further purification.

The $^{1}$H NMR spectra were recorded on a Bruker Avance spectrometer (400 MHz). Mass spectra were measured on a HP1100LC/MSD electrospray ionization mass spectrometry (ESI-MS). Elemental analysis was carried out on a Vario-EL analyser. Time-gated luminescence spectra and luminescence

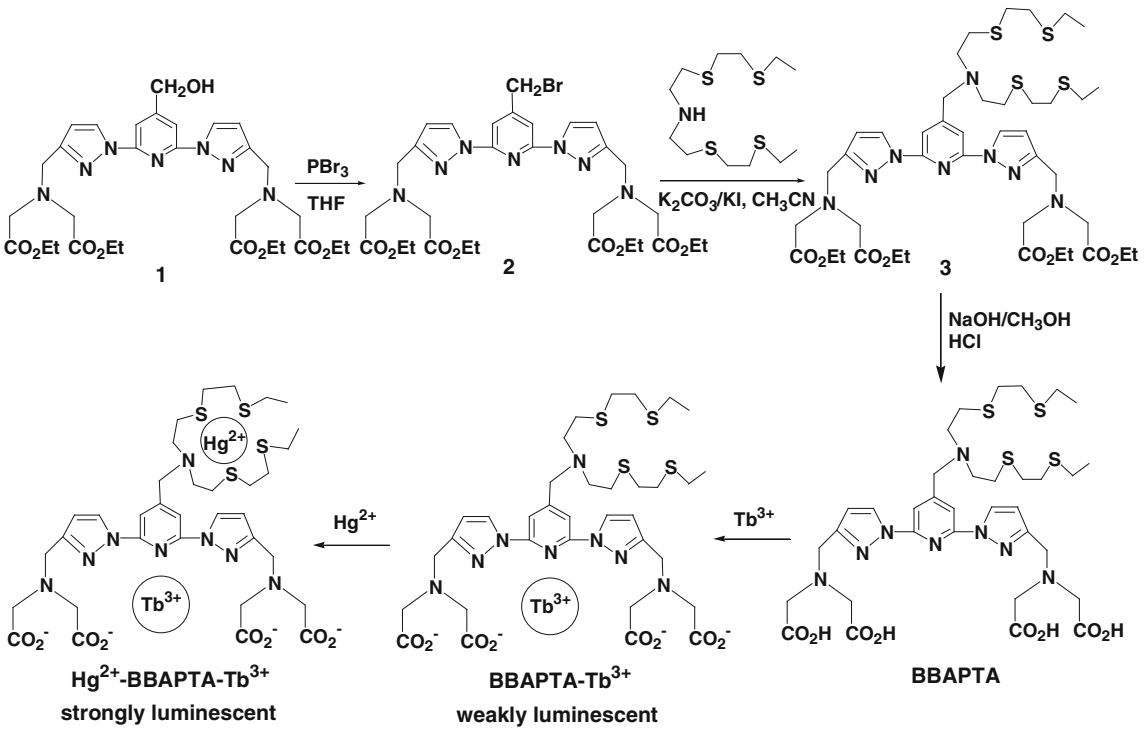


**Scheme 1** Synthesis procedure of the dual-functional ligand BBAPTA and its reactions with $Tb^{3+}$ and $Hg^{2+}$ ions

properties were measured on a Perkin-Elmer LS 50B luminescence spectrometer. The luminescence quantum yields ($\phi$) of BBAPTA-$Tb^{3+}$ and $Hg^{2+}$-BBAPTA-$Tb^{3+}$ were measured in a 0.05 M Tris-HCl buffer of pH 7.0 and calculated by using the equation $\phi_1=I_1\varepsilon_2C_2\phi_2/I_2\varepsilon_1C_1$ with a standard luminescence quantum yield of $\phi_2=0.10$ for the $Tb^{3+}$ complex of *N,N,N′,N′*-(4′-phenyl-2,2′:6′,2″-terpyridine-6,6″-diyl) bis(methylenenitrilo) tetrakis (acetate) ($\varepsilon_{337nm}$=14,000 $cm^{-1}$ $M^{-1}$) [28]. In the equation, $I_1$ and $I_2$, $\varepsilon_1$ and $\varepsilon_2$, $C_1$ and $C_2$ are the luminescence intensities, molar extinction coefficients, and concentrations for the measured complex and the standard complex, respectively. The time-gated luminescence measurement for the calibration curve was carried out on a Perkin-Elmer Victor 1420 multilabel counter with an excitation wavelength of 320 nm, emission wavelength of 545 nm, delay time of 0.2 ms, counting time of 0.4 ms, and cycling time of 1.0 ms.

## Synthesis of the Ligand

(i) Synthesis of tetraethyl *N,N,N′,N′*-[2,6-bis(3′-aminomethyl-1′-pyrazolyl)-4-bromomethyl- pyridine] tetrakis(acetate) (compound 2). To a solution of 0.69 g compound 1 (1.07 mmol) in 15 mL of dry THF was added dropwise 347 mg of $PBr_3$ (1.28 mmol). After the solution was stirred at room temperature for 2 h, 150 mL of $CHCl_3$ was added. The solution was washed with 100 mL of water, dried with $Na_2SO_4$, and then the solvent was evaporated. Purification by silica gel column chromatography with petroleum ether-ethyl acetate (2:1, v/v) as the eluent gave the compound 2 as a white oil (0.56 g, 73.7% yield). $^1$H NMR ($CDCl_3$): $\delta$=1.28 (t, 12H), 3.68 (s, 8H), 4.11 (s, 4H), 4.20(m, 8H), 4.47 (s, 2H), 6.60 (d, *J* =2.4 Hz, 2H), 7.82 (s, 2H), 8.48 (d, *J*=2.4 Hz, 2H).

(ii) Synthesis of tetraethyl *N,N,N′,N′*-{[2,6-bis(3′-aminomethyl-1′-pyrazolyl)-4- [*N,N*-bis(3″,6″-dithiaoctyl)-aminomethyl]-pyridine]} tetrakis(acetate) (compound 3). To a mixture of 266 mg TTM (0.85 mmol), 259 mg KI (1.56 mmol) and 216 mg $K_2CO_3$ (1.56 mmol) in 20 mL dry $CH_3CN$ was added a solution of 500 mg compound 2 (0.71 mmol) in 15 mL dry $CH_3CN$ under an argon atmosphere. The reaction mixture was refluxed for 24 h with stirring, and then cooled to room temperature. After the solvent was evaporated, the residue was dissolved in 100 mL $CH_2Cl_2$. The solution was washed with 100 mL of water, dried with $Na_2SO_4$, and then the solvent was evaporated. Purification by silica gel column chromatography with petroleum ether-ethyl acetate (3:2, v/v) as the eluent gave the compound 3 as a yellow oil (0.19 g, 28.7% yield). $^1$H NMR ($CDCl_3$): $\delta$=1.20–1.30 (m, 18H), 2.51 (m, 4H), 2.70 (m, 12H), 2.80 (t, 4H), 3.64 (s, 8H), 3.78 (s, 2H), 4.07 (s, 4H), 4.16–4.22 (m, 8H), 6.54 (d, 2H), 7.80 (s, 2H), 8.49 (d, 2H).

(iii) Synthesis of BBAPTA. A mixture of 0.19 g compound 3 (0.20 mmol), 0.25 g NaOH (6.25 mmol) and 25 mL methanol was stirred at room temperature for 24 h. After evaporation, the residue was dissolved in 3 mL water, and pH of the solution was adjusted to ~3 with 3 M HCl. The solution was stirred for 20 h at room temperature and the precipitate was collected by filtration. The dried precipitate was added to 30 mL of dry acetonitrile, and the mixture was refluxed for 30 min. After the precipitate was filtered and dried, BBAPTA was obtained as a brown solid (40 mg, 24.0% yield). $^1$H NMR (DMSO): $\delta$=1.10 (t, 6H), 2.44 (m, 4H), 2.65 (m, 12H), 2.71 (m, 4H), 3.47 (s, 8H), 3.86 (s, 2H), 3.94 (s, 4H), 6.54 (d, 2H), 7.75 (s, 2H), 8.52 (d, 2H). ESI-MS (*m/z*): calcd. for $C_{34}H_{50}N_8O_8S_4$, 826.3; found, 825.3 ([M-H]$^-$). Anal. calcd. for $C_{34}H_{50}N_8O_8S_4{\cdot}2NaCl{\cdot}2H_2O$: C, 41.70; H, 5.56; N, 11.44; found: C, 41.72; H, 5.37; N, 11.29.

## Luminescence Responses of BBAPTA-$Tb^{3+}$ to Different Metal Ions

The aqueous solutions of metal ions were prepared by dissolving $HgCl_2$, $Co(NO_3)_2{\cdot}6H_2O$, $MnSO_4{\cdot}H_2O$, $Cd(NO_3)_2{\cdot}2H_2O$, $PdCl_2{\cdot}2H_2O$, $Zn(NO_3)_2{\cdot}6H_2O$, $Ni(NO_3)_2{\cdot}6H_2O$, $Pb(NO_3)_2$, $Mg(NO_3)_2{\cdot}6H_2O$, $Ca(NO_3)_2$, $Ba(NO_3)_2$, $SnCl_2{\cdot}2H_2O$, $AgNO_3$, $Cu(NO_3)_2{\cdot}3H_2O$, $(NH_4)_2Fe(SO_4)_2{\cdot}6H_2O$, $Fe(NO_3)_3{\cdot}6H_2O$ in distilled water, respectively. The solution of BBAPTA-$Tb^{3+}$ was prepared by in-situ mixing equivalent molar of BBAPTA and $TbCl_3$ in 0.05 M HEPES buffer of pH 7.0. After different metal ions (5.0 μM) were added to the solution of BBAPTA-$Tb^{3+}$ (1.0 μM) with stirring, respectively, the solutions were incubated for 10 min at room temperature, and then subjected to the luminescence measurements.

## Time-Gated Luminescence Detection of $Hg^{2+}$

The solution of BBAPTA-$Tb^{3+}$ was prepared by mixing equivalent molar of BBAPTA and $TbCl_3$ in 0.05 M Tris-HCl buffer of pH 7.0. After different concentrations of $HgCl_2$ were added to the solution of BBAPTA-$Tb^{3+}$ (1.0 μM), respectively, the solutions were stirred for 0.5 h at room temperature, and then subjected to the time-gated luminescence spectrum measurements on the LS 50B luminescence spectrometer. For the measurement of calibration curve, the solutions of BBAPTA-$Tb^{3+}$ (0.1 μM) added with different concentrations of $HgCl_2$ ($10^{-5}$–$10^{-7}$ M) were added to the wells of a 96-well microtiter plate (50 μL per well)

respectively, and then subjected to the time-gated luminescence measurement on the Victor 1420 multilabel counter.

## Results and Discussion

### Design and Synthesis of the Probe

Differently from the fluorescence of organic dyes, the luminescence of lanthanide (mainly $Eu^{3+}$ and $Tb^{3+}$) complexes has several very unique luminescence properties including large Stokes shift, long luminescence lifetime and sharp emission profile. These properties have allowed the complexes to be used as luminescent probes for the background-free time-gated luminescence detections of some analytes in complicated environmental and biological samples [29–31], since the fast decaying autofluorescence and scattering lights can be effectively eliminated by the time-gated detection mode. To develop the application of time-gated luminescence assay technique, the essential objective is the developments of various functional lanthanide probes that can selectively recognize the target analytes to give the long-lived luminescence responses. However, although some lanthanide complex-based luminescent probes that can be used for time-gated luminescence detections of some small molecules and ions, such as singlet oxygen [32], $H_2O_2$ [33, 34], peroxynitrite [35], hydroxyl radical [36], nitric oxide [37], and $Zn^{2+}$ [27], have been reported in recent several years, compared to various organic dye-based fluorescent probes, the lanthanide complex-based luminescent probes are still very limited because the mechanism of lanthanide luminescence is more complicated than that of the organic dye's fluorescence, and thereby, the probe design is more difficult.

In this work, a novel dual-functional ligand BBAPTA was designed by comprehensively considering its antenna capability for sensitizing the $Tb^{3+}$ luminescence and its recognition capability for $Hg^{2+}$ ions in aqueous solutions. In the ligand, the moiety of 2,6-bis(N-pyrazolyl) pyridine polyacid derivative was chosen as a $Tb^{3+}$ luminescence antenna due to its good water solubility, high chelating affinity to $Tb^{3+}$ (nonadentate coordination), and excellent antenna capability for sensitizing the $Tb^{3+}$ luminescence [23–25]. The TTM moiety in the ligand has two functions. One is to quench the $Tb^{3+}$ luminescence via a PET process to make the $Tb^{3+}$ luminescence be turned-off, and the other is to enable the ligand to have a function to selectively recognize $Hg^{2+}$ ions. Thus, when the weakly luminescent BBAPTA-$Tb^{3+}$ complex is reacted with $Hg^{2+}$, accompanied by the coordination of the TTM moiety to $Hg^{2+}$, the PET process from TTM to the $Tb^{3+}$ complex moiety is inhibited, and the $Tb^{3+}$ luminescence is turned-on.

Scheme 1 shows the synthesis procedure of the dual-functional ligand BBAPTA and its reactions with $Tb^{3+}$ and $Hg^{2+}$ ions. This ligand was synthesized with three-step reactions by coupling a 2,6-bis(N-pyrazolyl) pyridine polyacid derivative with TTM. At first, the tetraethyl ester derivative of 2,6-bis(N-pyrazolyl)-4-bromomethyl-pyridine tetrakis(acetate) (compound 2) was synthesized by reacting compound 1 with $PBr_3$ in anhydrous THF. After it was reacted with TTM in dry $CH_3CN$ in the presence of $K_2CO_3$ and KI under an argon atmosphere, the tetraethyl ester derivative of BBAPTA (compound 3) was obtained. Finally, BBAPTA was obtained by the hydrolysis and neutralization of compound 3 with NaOH-methanol and aqueous HCl, respectively. The structure and composition of BBAPTA were well characterized by the NMR, ESI-MS and elementary analyses.

### Luminescence Properties of the Probe

The luminescence properties of BBAPTA-$Tb^{3+}$ were measured in a 0.05 M Tris-HCl buffer of pH 7.0. This $Tb^{3+}$ complex shows the maximum absorption and emission wavelengths at 306 nm ($\varepsilon = 1.71 \times 10^4\ M^{-1} cm^{-1}$) and 540 nm, respectively. As expected, the luminescence of BBAPTA-$Tb^{3+}$ was very weak with a low luminescence quantum yield ($\phi$=0.33%±0.02%, $\tau$=3.22 ms). However, upon addition of 1.0 equiv of $Hg^{2+}$, the luminescence quantum yield of the solution was ~5-fold increased ($\phi$=1.65%±0.17%) with a long luminescence lifetime ($\tau$=3.14 ms). This result indicates that the TTM moiety in BBAPTA-$Tb^{3+}$ can display an "off/on" luminescence switch for the recognition of $Hg^{2+}$ ions. Figure 1 shows the time-gated excitation and emission spectra of BBAPTA-$Tb^{3+}$ in the absence and presence of $Hg^{2+}$ ions in 0.05 M Tris-HCl buffer of pH 7.0. The spectra show the typical $Tb^{3+}$ emission pattern with a main emission peak at 540 nm and several side peaks centred at 488, 581, 619, and 642 nm, respectively.

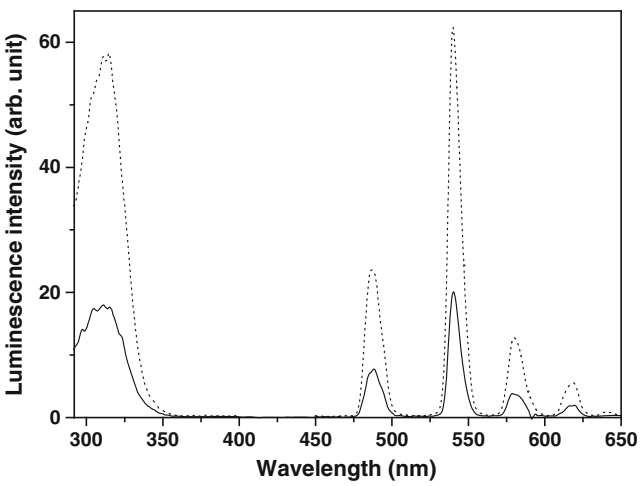


**Fig. 1** Time-gated excitation and emission spectra of BBAPTA-$Tb^{3+}$ (1.0 μM) in the absence (solid lines) and presence (dot lines) of $Hg^{2+}$ (5.0 μM)

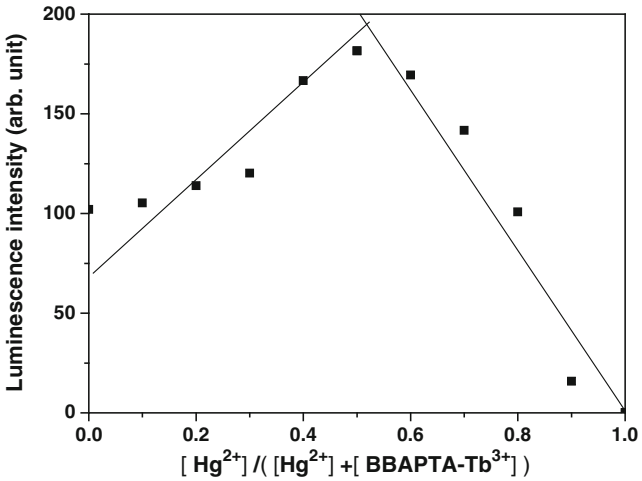


**Fig. 2** Job's plot of the reaction between BBAPTA-$Tb^{3+}$ and $Hg^{2+}$ in 0.05 M Tris-HCl buffer of pH 7.0. The total concentrations of BBAPTA-$Tb^{3+}$ and $Hg^{2+}$ were kept at 10 μM

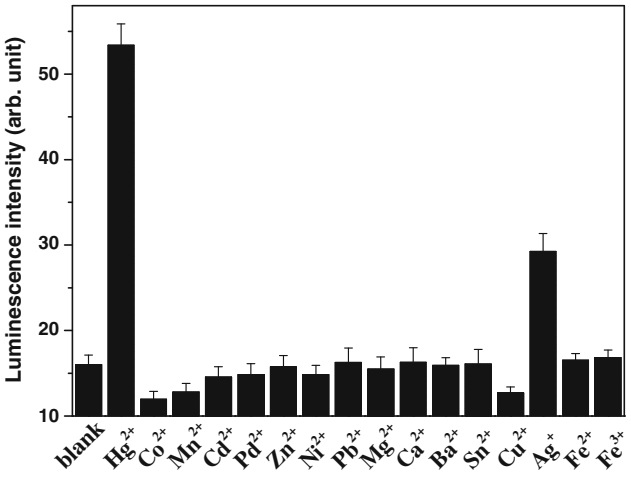


**Fig. 4** Time-gated luminescence intensity responses of BBAPTA-$Tb^{3+}$ (1.0 μM) to different metal ions (5.0 μM) in 0.05 M HEPES buffer of pH 7.0

To further confirm the formation of the heterobimetallic complex $Hg^{2+}$-BBAPTA-$Tb^{3+}$ in the buffer, the reaction of BBAPTA-$Tb^{3+}$ with $Hg^{2+}$ was investigated by the Job's plotting analysis. As shown in Fig. 2, the Job's plot between the reaction of BBAPTA-$Tb^{3+}$ and $Hg^{2+}$ exhibits a maximum at 0.5 molecular fraction, which indicates that BBAPTA-$Tb^{3+}$ can bind with $Hg^{2+}$ with a 1:1 stoichiometry.

## Time-Gated Luminescence Detection of $Hg^{2+}$ Using BBAPTA-$Tb^{3+}$ as a Probe

Before the detection, the effects of pH on the luminescence intensities of BBAPTA-$Tb^{3+}$ and $Hg^{2+}$-BBAPTA-$Tb^{3+}$ as well as the luminescence response specificity of BBAPTA-$Tb^{3+}$ to $Hg^{2+}$ were investigated. Figure 3 shows the luminescence intensities of BBAPTA-$Tb^{3+}$ and $Hg^{2+}$-BBAPTA-$Tb^{3+}$ in 0.05 M Tris-HCl buffers at different pHs ranging from 3.0 to 10.0. It can be observed that the luminescence intensities of BBAPTA-$Tb^{3+}$ and $Hg^{2+}$-BBAPTA-$Tb^{3+}$ display quite different behaviors against the pH changes: the gradual luminescence increase of BBAPTA-$Tb^{3+}$ with the decrease of pH at acidic pHs, and the gradual luminescence decrease of $Hg^{2+}$-BBAPTA-$Tb^{3+}$ with the increase of pH at basic pHs . These phenomena can be explained by the fact that, the luminescence increase of BBAPTA-$Tb^{3+}$ at acidic pHs is due to the protonation of the tertiary amine of TTM, since which can result in the

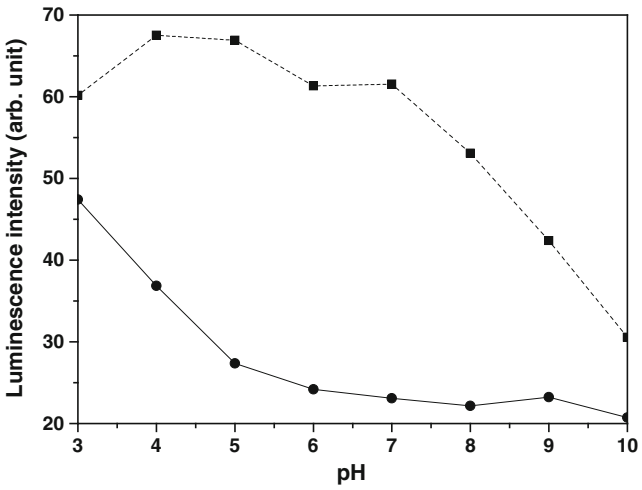


**Fig. 3** Effects of pH on the luminescence intensities of BBAPTA-$Tb^{3+}$ (1.0 μM) in the absence (solid line) and presence (dash line) of $Hg^{2+}$ (5.0 μM) in 0.05 M Tris-HCl buffers with different pHs

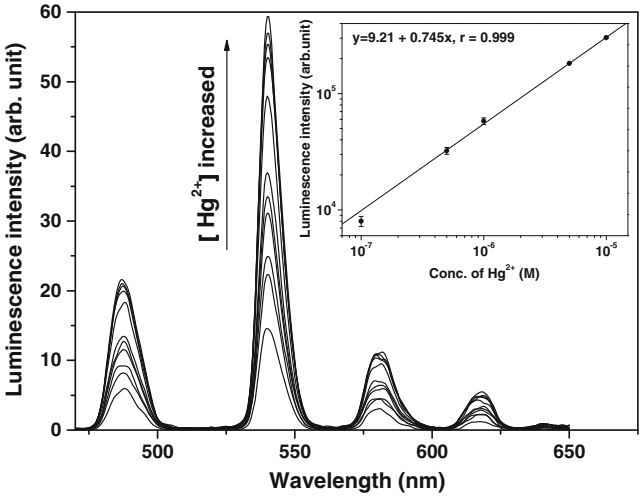


**Fig. 5** Time-gated emission spectra (measured on the Perkin-Elmer LS 50B spectrometer) of BBAPTA-$Tb^{3+}$ (1.0 μM) in the presence of different concentrations of $Hg^{2+}$ (0.0, 0.2, 0.4, 0.6, 0.8, 1.0, 2.0, 4.0, 6.0, 8.0, 10 μM). The inset is the calibration curve for the time-gated luminescence detection of $Hg^{2+}$ (0.1–10 μM) using BBAPTA-$Tb^{3+}$ (0.1 μM) as a probe (measured on a Perkin-Elmer Victor 1420 multilabel counter)

decrease of the PET efficiency of the TTM moiety, while the luminescence decrease of $Hg^{2+}$-BBAPTA-$Tb^{3+}$ at basic pHs is due to the hydrolysis of $Hg^{2+}$, since which can cause the dissociation of $Hg^{2+}$-BBAPTA-$Tb^{3+}$ by the formation of Hg(II) hydroxides. Because the maximum and stable luminescence intensity ratio of $Hg^{2+}$-BBAPTA-$Tb^{3+}$ to BBAPTA-$Tb^{3+}$ is in the range of pH 6–7, the pH value of 7.0 can be considered to be the optimal pH for the luminescence detection of $Hg^{2+}$ ions.

The luminescence responses of BBAPTA-$Tb^{3+}$ to various metal ions were examined in 0.05 M HEPES buffer of pH 7.0 by adding different metal ions into the BBAPTA-$Tb^{3+}$ solution, respectively (the HEPES buffer was used instead of the Tris-HCl buffer to avoid the reaction of the buffer with $Ag^{+}$ ions). As shown in Fig. 4, the luminescence intensity of BBAPTA-$Tb^{3+}$ was significantly increased upon the addition of $Hg^{2+}$, whereas almost no luminescence responses of BBAPTA-$Tb^{3+}$ to the additions of $Co^{2+}$, $Mn^{2+}$, $Cd^{2+}$, $Pd^{2+}$, $Zn^{2+}$, $Ni^{2+}$, $Pb^{2+}$, $Mg^{2+}$, $Ca^{2+}$, $Ba^{2+}$, $Sn^{2+}$, $Cu^{2+}$, $Fe^{2+}$, $Fe^{3+}$ were observed. This selective turn-on luminescence response of BBAPTA-$Tb^{3+}$ to $Hg^{2+}$ demonstrates that BBAPTA-$Tb^{3+}$ is a highly specific luminescent probe for the detection of $Hg^{2+}$ in aqueous solutions. It should be mentioned that although $Ag^{+}$ can also induce the increase of the luminescence intensity, its effect can be easily eliminated by using a $Cl^{-}$ containing buffer, such as Tris-HCl buffer, as the detection medium.

Based on the above results, a quantitative time-gated luminescence titration of $Hg^{2+}$ was conducted using BBAPTA-$Tb^{3+}$ as a probe by adding different concentrations of $Hg^{2+}$ into the solution of BBAPTA-$Tb^{3+}$ in 0.05 M Tris-HCl buffer of pH 7.0. As shown in Fig. 5, the luminescence spectrum of the probe shows a sensitive response to the addition of $Hg^{2+}$ ions. Moreover, the dose-dependent luminescence enhancement shows a good linearity that can be expressed as log (signal)=0.745 log[$Hg^{2+}$] +9.21 ($r$=0.999) in the concentration range of 0.1 μM to 10 μM (the inset in Fig. 5). The detection limit for $Hg^{2+}$, calculated as the concentration corresponding to three standard deviations of the background signal, is 17 nM, which indicates that BBAPTA-$Tb^{3+}$ can be used as a sensitive luminescence probe for the quantitative time-gated luminescence detection of trace $Hg^{2+}$ ions in aqueous solutions.

## Conclusions

In summary, we described here the design and synthesis of a $Tb^{3+}$ complex-based luminescent probe for the recognition and time-gated luminescence detection of $Hg^{2+}$ ions in aqueous solutions. This probe was designed and synthesized based on the PET mechanism by incorporating a $Tb^{3+}$ complex of 2,6-bis(N-pyrazolyl)pyridine polyacid derivative into a $Hg^{2+}$-recognition moiety TTM. Compared to the organic dye-based fluorescent probes, the new probe has several very desirable properties including long emission lifetime, large stokes shift, high selectivity, and excellent water solubility and stability, which provides a favorably useful method for the luminescent detection of $Hg^{2+}$ ions in complicated environmental and biological samples since the background noises can be easily deleted by the time-gated detection mode.

**Acknowledgement** The present work was supported by the National Natural Science Foundation of China (Nos. 20835001, 20975017, 20923006).

## References

1. Clarkson TW, Magos L, Myers GJ (2003) The toxicology of mercury-current exposures and clinical manifestations. N Engl J Med 349:1731–1737
2. Guzzi G, La Porta CAM (2008) Molecular mechanisms triggered by mercury. Toxicology 244:1–12
3. Lee MH, Lee SW, Kim SH, Kang C, Kim JS (2009) Nanomolar Hg(II) detection using nile blue chemodosimeter in biological media. Org Lett 11:2101–2104
4. Grandjean P, Weihe P, White RF, Debes F (1998) Cognitive performance of children prenatally exposed to 'safe' levels of methylmercury. Environ Res 77:165–172
5. Harada M (1995) Minamata disease: methylmercury poisoning in Japan caused by environmental pollution. Crit Rev Toxicol 25:1–24
6. Romero T, Caballero A, Espinosa A, Tárraga A, Molina P (2009) A multiresponsive two-arm ferrocene-based chemosensor molecule for selective detection of mercury. Dalton Trans 12:2121–2129
7. Malm O (1998) Gold mining as a source of mercury exposure in the Brazilian Amazon. Environ Res 77:73–78
8. Renzoni A, Zino F, Franchi E (1998) Mercury levels along the food chain and risk for exposed populations. Environ Res 77:68–72
9. Gustin MS, Coolbaugh MF, Engle MA, Fitzgerald BC, Keislar RE, Lindberg SE, Nacht DM, Quashnick J, Rytuba JJ, Sladek C, Zhang H, Zehner RE (2003) Atmospheric mercury emissions from mine wastes and surrounding geologically enriched terrains. Environ Geol 43:339–351
10. Chu P, Porcella DB (1995) Mercury stack emissions from USA electricutility power plants. Water Air Soil Pollut 80:135–144
11. Ramalhosa E, Río Segade S, Pereira E, Vale C, Duarte A (2001) Simple methodology for methylmercury and inorganic mercury determinations by high-performance liquid chromatography–cold vapour atomic fluorescence spectrometry. Anal Chim Acta 448:135–143
12. Yang L, Mester Z, Sturgeon RE (2003) Determination of methyl mercury in fish tissues by isotope dilution SPME-GC-ICP-MS. J Anal At Spectrom 18:431–436
13. Reyes LH, Rahman GM, Kingston HM (2009) Robust microwave-assisted extraction protocol for determination of total mercury and methylmercury in fish tissues. Anal Chim Acta 631:121–128
14. Climent E, Marcos MD, Martínez-Máñez R, Sancenón F, Soto J, Rurack K, Amorós P (2009) The determination of methylmercury in real samples using organically capped mesoporous inorganic

materials capable of signal amplification. Angew Chem Int Ed 48:8519–8522
15. Nolan EM, Lippard SJ (2008) Tools and tactics for the optical detection of mercuric ion. Chem Rev 108:3443–3480
16. Nolan EM, Lippard SJ (2007) Turn-On and ratiometric mercury sensing in water with a red-emitting probe. J Am Chem Soc 129:5910–5918
17. Xie JP, Zheng YG, Ying JY (2010) Highly selective and ultrasensitive detection of $Hg^{2+}$ based on fluorescence quenching of Au nanoclusters by $Hg^{2+}$-$Au^{+}$ interactions. Chem Commun 46:961–963
18. Lim CS, Kang DW, Tian YS, Han JH, Hwang HL, Cho BR (2010) Detection of mercury in fish organs with a two-photon fluorescent probe. Chem Commun 46:2388–2390
19. Du JJ, Fan JL, Peng XJ, Sun PP, Wang JY, Li HL, Sun SG (2010) A new fluorescent chemodosimeter for $Hg^{2+}$: selectivity, sensitivity, and resistance to Cys and GSH. Org Lett 12:476–479
20. Bhalla V, Tejpal R, Kumar M, Sethi A (2009) Terphenyl derivatives as "turn on" fluorescent sensors for mercury. Inorg Chem 48:11677–11684
21. Zhang XL, Xiao Y, Qian XH (2008) A ratiometric fluorescent probe based on FRET for imaging $Hg^{2+}$ ions in living cells. Angew Chem Int Ed 47:8025–8029
22. Li HW, Li Y, Dang YQ, Ma LJ, Wu YQ, Hou GF, Wu LX (2009) An easily prepared hypersensitive water-soluble fluorescent probe for mercury(II) ions. Chem Commun 45:4453–4455
23. Yuan JL, Wang GL, Majima K, Matsumoto K (2001) Synthesis of a terbium fluorescent chelate and its application to time-resolved fluoroimmunoassay. Anal Chem 73:1869–1876
24. Brunet E, Juanes O, Sedano R, Rodríguez-Ubis JC (2002) Lanthanide complexes of polycarboxylate-bearing dipyrazolylpyridine ligands with near-unity luminescence quantum yields: the effect of pyridine substitution. Photochem Photobiol Sci 1: 613–618
25. Kadjane P, Starck M, Camerel F, Hill D, Hildebrandt N, Ziessel R, Charbonnière LJ (2009) Divergent approach to a large variety of versatile luminescent lanthanide complexes. Inorg Chem 48:4601–4603
26. Zeng L, Miller EW, Pralle A, Isacoff EY, Chang CJ (2006) A selective turn-on fluorescent sensor for imaging copper in living cells. J Am Chem Soc 128:10–11
27. Ye ZQ, Wang GL, Chen JX, Fu XY, Zhang WZ, Yuan JL (2010) Development of a novel terbium chelate-based luminescent chemosensor for time-resolved luminescence detection of intracellular $Zn^{2+}$ ions. Biosens Bioelectron 26:1043–1048
28. Latva M, Takalo H, Mukkala VM, Matachescu C, Rodríguez-Ubis JC, Kankare J (1997) Correlation between the lowest triplet state energy level of the ligand and lanthanide(III) luminescence quantum yield. J Lumin 75:149–169
29. Wu J, Ye ZQ, Wang GL, Jin DY, Yuan JL, Guan YF, Piper J (2009) Visible-light-sensitized highly luminescent europium nanoparticles: preparation and application for time-gated luminescence bioimaging. J Mater Chem 19:1258–1264
30. Eliseeva SV, Bünzli JCG (2010) Lanthanide luminescence for functional materials and bio-sciences. Chem Soc Rev 39:189–227
31. Bünzli JCG (2010) Lanthanide luminescence for biomedical analyses and imaging. Chem Rev 110:2729–2755
32. Song B, Wang GL, Tan MQ, Yuan JL (2006) A europium(III) complex as an efficient singlet oxygen luminescence probe. J Am Chem Soc 128:13442–13450
33. Lippert AR, Gschneidtner T, Chang CJ (2010) Lanthanide-based luminescent probes for selective time-gated detection of hydrogen peroxide in water and in living cells. Chem Commun 46:7510–7512
34. Ye ZQ, Chen JX, Wang GL, Yuan JL (2011) Development of a terbium complex-based luminescent probe for imaging endogenous hydrogen peroxide generation in plant tissues. Anal Chem 83:4163–4169
35. Song CH, Ye ZQ, Wang GL, Yuan JL, Guan YF (2010) A lanthanide complex-based ratiometric luminescent probe specific for peroxynitrite. Chem Eur J 16:6464–6472
36. Cui GF, Ye ZQ, Chen JX, Wang GL, Yuan JL (2011) Development of a novel terbium(III) chelate-based luminescent probe for highly sensitive time-resolved luminescence detection of hydroxyl radical. Talanta 84:971–976
37. Chen YG, Guo WH, Ye ZQ, Wang GL, Yuan JL (2011) A europium(III) chelate as an efficient time-gated luminescent probe for nitric oxide. Chem Commun 47:6266–6268